Journal Pre-proof

Processes driving seagrass soils composition along the western Mediterranean: the case of the southeast Iberian Peninsula

Nerea Piñeiro-Juncal, Elena Diaz-Almela, Carmen Leiva-Dueñas, Ona Deulofeu, Jaime Frigola, Montserrat Soler, Antonio Martinez-Cortizas, Santiago Giralt, Jordi Garcia-Orellana, Miguel Ángel Mateo

PII: S0048-9697(20)37883-9

DOI: https://doi.org/10.1016/j.scitotenv.2020.144352

Reference: STOTEN 144352

To appear in: *Science of the Total Environment*

Received date: 17 June 2020

Revised date: 5 November 2020

Accepted date: 2 December 2020

Please cite this article as: N. Piñeiro-Juncal, E. Diaz-Almela, C. Leiva-Dueñas, et al., Processes driving seagrass soils composition along the western Mediterranean: the case of the southeast Iberian Peninsula, *Science of the Total Environment* (2020), https://doi.org/10.1016/j.scitotenv.2020.144352

This is a PDF file of an article that has undergone enhancements after acceptance, such as the addition of a cover page and metadata, and formatting for readability, but it is not yet the definitive version of record. This version will undergo additional copyediting, typesetting and review before it is published in its final form, but we are providing this version to give early visibility of the article. Please note that, during the production process, errors may be discovered which could affect the content, and all legal disclaimers that apply to the journal pertain.

© 2020 Published by Elsevier.

Journal Pre-proof

Title: Processes driving seagrass soils composition along the western Mediterranean: the case of the southeast Iberian Peninsula

Authors: Nerea Piñeiro-Juncal [1,2]*, Elena Diaz-Almela[2], Carmen Leiva-Dueñas[2], Ona Deulofeu[2], Jaime Frigola[3], Montserrat Soler[2], Antonio Martinez-Cortizas[1], Santiago Giralt[5], Jordi Garcia-Orellana[5,6], and Miguel Ángel Mateo[2,7].

[1] EcoPast (GI-1553), Facultade de Bioloxía, Universidade de Santiago de Compostela, Campus Sur s/n, Santiago de Compostela, 15782, Spain

[2] Group of Aquatic Macrophytes Ecology, Centre d'Estudis Avançats de Blanes (CEAB-CSIC), 17300 – Blanes, Girona, Spain

[3] GRC Geociències Marines, Departament de Dinàmica de la Terra i de l'Oceà, Facultat de Ciències de la Terra, Universitat de Barcelona, Carrer Martí i Franquès s/n, 08028 Barcelona, Spain

[4] Geosciences Barcelona (Geo3BCN-CSIC), Lluís Solé i Sabarís s/n, 08028 Barcelona, Spain

[5] Institut de Ciència i Tecnologia Ambientals, Universitat Autònoma de Barcelona, 08193 Cerdanyola del Vallès, Barcelona, Spain

[6] Departament de Física, Universitat Autònoma de Barcelona, 08193 Cerdanyola del Vallès, Barcelona, Spain

[7] Centre for Marine Ecosystems Research, Edith Cowan University, Joondalup, WA, Australia

*Corresponding author: Nerea Piñeiro-Juncal

np.juncal@gmail.com

EcoPast (GI-1553), Facultade de Bioloxía, Universidade de Santiago de Compostela, Campus Sur s/n, Santiago de Compostela, 15782, Spain

Running title: Formation processes of seagrass soils

1. Introduction

Seagrasses are a polyphyletic group of aquatic angiosperms that colonize coastal areas of all continents except Antarctica (Hartog and Kuo, 2006). They can settle from intertidal areas to several meters deep in the subtidal, depending on local factors such as light availability and coastal hydrodynamics (Duarte, 1991; Koch, 2001). They are known to promote sedimentation by reducing the hydrodynamic forces, directly trapping suspended particles (Agawin and Duarte, 2002; Hendriks et al., 2008; Gruber and Kemp, 2010; Hansen and Reidenbach, 2012) and by avoiding particle-resuspension (Terrados and Duarte, 2000; Gacia and Duarte, 2001; Hendriks et al., 2010), forming well-ordered deposits than can be used as environmental archives (Mateo et al., 2002, 2010; Serrano et al., 2016a; López-Merino et al., 2017). Nevertheless, seagrass substrates are continuously modified by the overlaying living plants, which can change soil characteristics such as texture (Rueda et al., 2008; van Katwijk et al., 2010), composition (Kennedy et al., 2004; Smit et al., 2005; Fourqurean et al., 2012a; Mazarrasa et al., 2015) or redox conditions (Duarte et al., 2005). Plant derived changes in the substrate are held in the rhizosphere and can vary with meadow maturity (Holmer, 2018). Rhizosphere depth differs largely between species but is usually restricted to the uppermost 40 cm of the marine sedimentary floor. It has been reported that it occupies from 3 to 80% of the substrate volume and has a total absorptive area often exceeding 1 m^2 m^{-2} (Duarte et al., 2005a). The rhizomes and roots of seagrass release O_2, generating oxic microenvironments and preventing the formation of phytotoxins (Borum et al., 2006; Jensen et al., 2007), and OM which promotes microbial activity (Mateo et al., 2006).

Over the last decade, great attention has been paid to the role of these meadows as chemical filters, especially as CO_2 sinks (Romero et al., 1994; Duarte et al., 2005b; Fernandes et al., 2009; Serrano et al., 2011; Fourqurean et al., 2012a). Organic matter (OM) accumulates in seagrass soils

because of (1) particles-trapping and deposition favored by the seagrass canopy, (2) limited mineralization due to the anoxic conditions in the soil and (3) the refractory nature of the seagrass tissues, which can be preserved over millennia (Mateo et al., 1997; Lavery et al., 2013; Serrano et al., 2016b). The carbon sequestered in these ecosystems, together with mangroves and salt marshes, is known as blue carbon (Nellemann et al., 2009) and represents close to half of the carbon buried in the ocean floor, despite seagrasses covering less than 2% of the ocean extension (Duarte et al., 2005b).

The particular physicochemical characteristics of the soil would vary according to environmental factors operating in the course of its development (e.g. Cebrian et al., 2000; Mazarrasa et al., 2015). Demas and Rabenhorst (2001) propose a combination of factors affecting subaqueous soils formation: climatic temperature regime, organisms, bathymetry, flow regime, parent material, time, water column attributes and catastrophic events. Several of these factors have been found to have an impact on seagrass soils (e.g. Thomson et al., 2019; Alcoverro et al., 1997). Their biogeochemistry has been largely studied by marine scientist (e.g., Holmer, 2018; Marbà et al., 2006). However, the available information focuses mainly in the uppermost part of the soils, where the rhizosphere is found. In the present work, we apply principal component analysis to summarize the information about soil composition and to explore the main geochemical signals in seagrass soils from the two most abundant seagrass species in the Mediterranean Sea, encompassing both rhizosphere and subsoil. To this end, we analyzed 15 soil cores from meadows along ca. 350 km of the Southern coast of the Iberian Peninsula, allowing us to characterize the common processes driving their geochemical composition. Understanding these common geochemical processes can shed some light into the role of marine meadows soils as blue carbon sinks as well as environmental archives.

Journal Pre-proof

2. Site description and methods

2.1. Study area

We sampled 15 stations in seagrass meadows along a ca. 350 km stretch of the eastern Andalusian coast, southeast of the Iberian Peninsula, where outcrops of volcanic, metamorphic, and sedimentary rocks can be found (Red de Información Ambiental de Andalucia, 2020) (Fig. 1). The most abundant seagrass species in these coasts are *Posidonia oceanica* and *Cymodocea nodosa* (Luque and González, 2004). *Posidonia oceanica* is a slow-growing species with high biomass and productivity, that can colonize both sandy and rocky bottoms, often forming thick lignin-rich biogenic reefs, called "mat" (Boudouresque and Meinesz, 1982; Kaal et al., 2016), and whose meadows are considered a climax community. *Cymodocea nodosa* is a pioneer species that usually grows over sandy and muddy bottoms and can be found growing over degraded or dead *P. oceanica* meadows (Luque and González, 2004).

Fifteen stations distributed in 9 locations were sampled: Melicena (ME.S), Almerimar (AL.S), Roquetas (RO.S, RO.S-C and RO.S-CN), El Alquián (BA.S), Aguamarga (AG.S, AG.I and AG.D), Palomares (PA.I), Villaricos (DE.I), Terreros (TE.S and TE.D), and Calaburras (CA.S-C and CA.S-CN) (Table 1). These stations were selected to maximize bathymetry range, species and conservation status variability. At least three cores were retrieved per station, among which the longest was selected for this study (Table 1, Fig. 2). The stations were located in monospecific meadows of *P. oceanica* or *C. nodosa*, at water column depths ranging from 0.5 to 18.5 m (Table 1). The cores collected in El Alquián, Palomares and one from Roquetas (ROS.CN) belong to *C. nodosa* meadows. Both El Alquián and Palomares cores were retrieved in extensive well-formed meadows while ROS.CN core was sampled from a small lagoon formed between a *P. oceanica* reef and the shore (Moreno and Guirado, 2003). The remaining cores were sampled in *P. oceanica* meadows. Aguamarga and Terreros meadows were sampled at more than one water depth. In Aguamarga,

stations were located at shallow (AG.S, 4.8 m), intermediate (AG.I, 10.8 m) and deep (AG.D, 18 m) waters, while in Terreros cores were only obtained at shallow (TE.S, 5.5 m) and deep (TE.D, 18.5 m) ones. Two cores were sampled in degraded meadows: Villaricos (DE.I) and Melicena (ME.S). The meadow at Villaricos is in an advanced state of degradation, with a very low shoot density, high shoot mortality rate and extensive areas of dead mats (areas where plant cover has been lost). The Villaricos meadow is highly degraded mainly due to the influence of wastewater from a chemical plant that manufactures ethyl derivatives, among others, since the late 1960s (Moreno et al., 2001; Marbà et al., 2015; Consejería de Agricultura Ganadería Pesca y Desarrollo Sostenible, 2017). Although a waste water treatment plant was installed in 1999, the meadow is still declining, because either the water treatment is not efficient enough, and/or the pollutants trapped in the soil are still being processed by the plants (Agustín Barrajón and Diego Moreno, personal communication, technicians of the Andalusian Government Environment and Water Agency, AMAyA). The Melicena station is located in a degraded meadow, adjacent to an area where dead meadow has been observed, very likely related to an uncontrolled release of agriculture waste waters and sediments (Consejería de Agricultura Ganadería Pesca y Desarrollo Sostenible, 2017). We also sampled two dead *P. oceanica* meadows in Roquetas (RO.S-C) and in Calaburras (CA.S). In Calaburras two stations were recovered, one over a dead mat area covered with algae, and another over dead mat overgrown by *C. nodosa* (CA.S-C and CA.S-CN, respectively). Two different climatic areas can be found in the sampled coast. The Terreros, Villaricos, Palomares, Aguamarga, Alquian, Roquetas and Almerimar locations belong to a subdesertic Mediteranean climate (mean annual temperature of 17.6 °C), while the Calaburras and Melicena locations belong to a subtropical climate (mean annual temperature of 17.2 °C) with more abundant annual precipitations (CAGPDS, 2014; Leiva-Dueñas et al., 2021).

2.2. Sampling and laboratory methods

Cores were retrieved over the course of two sampling campaigns in October 2016 and 2017. All cores, except that at station TE.D (Table 1) were sampled by gently hammering and slowly rotating a PVC tube (150-200 cm long, internal diameter 7.5 cm) into the soil in SCUBA diving. The tube had a core catcher fitted at its bottom end to avoid loss of material during its retrieval. Core compaction was observed, and core-length corrections were done as described below. The core at station TE.D was taken using a vibrocore (Geo-Corer 3000, Igeotest) into a plastic core pipe (600 cm long, internal diameter 10 cm).

Cores were halved longitudinally in the laboratory. One of the halves was imaged and analyzed by non-destructive techniques at 1 cm steps at the CORELAB laboratory of the University of Barcelona. The elemental geochemical composition of the soil - aluminum (Al), silicon (Si), sulfur (S), chlorine (Cl), potassium (K), calcium (Ca), titanium (Ti), manganese (Mn), iron (Fe), nickel (Ni), zinc (Zn), bromine (Br), rubidium (Rb), strontium (Sr), zirconium (Zr) and lead (Pb) concentrations - was obtained by means of an Avaatech XRF-core scanner. Magnetic susceptibility (MS) was obtained with a Bartington Instruments MS2E point sensor mounted on a Geotek Multi-Sensor Core Logger. Some sections along the core, especially at the top, were impossible to measure by XRF or MS owing to their intrinsic nature (presence of plant macro-debris, shells or stones): AG.I 0-16 cm; AG.D 0-10 cm; DE.I 14-18 cm; TE.S 0-20 cm; AL.S 0-8 cm; ME.S 0-8 cm; RO.S 0-18 cm; RO.S-C 0-13 cm; CA.S 0-15 cm; CA.S-CN 0-30 cm; RO.S-CN 0-22 cm; PA.I 1-14, 44-50, 62-65, 77-89, 96-101 and 105-109 cm; and BA.S 0-7 and 57-96 cm. Afterwards, this half core was stored in a dark cold room at 4 °C as a backup, while the other half was used for further analyses. The analyzed half was subsampled every other 2 cm and the samples dried at 60 °C for four days. The vibrocore, TE.D, was subsampled every 10 cm, by recovering 20 ml with 3 cm wide un-capped plastic syringes. Even samples were measured for grain size distribution and total organic carbon (C_{org}). Grain size was determined by digesting the samples with hydrogen peroxide at 30% to remove the

OM, sieved at <1 mm and measured using laser diffraction (Mastersizer2000, Malvern Instruments, Centre d'Estudis Avançats de Blanes). The grain size fractions obtained were clay (<0.002 mm), silts (0.002-0.050 mm) and fine (0.05-0.50 mm, FSand), medium (0.5-1.0 mm, MSand) and coarse (>1 mm, CSand) sand. Samples for C_{org} were ground using an agate mortar (Mortar Grinder RM-200 RETSCH) and measured by mass-loss-on-ignition technique (450 °C for 5 h) to obtain the OM%. In 10 to 12 subsamples per core, around 1 g of ground sample was digested by adding HCl 1M to eliminate carbonates, centrifuged and rinsed with distilled water until pH ≈7 before drying at 60°C. The digested sample aliquot was used to measure C_{org} at the IACT-CSIC center in Granada using an elemental analyzer NA 1500 2 (Carlo Erba).

2.3. Dating and age-depth models

Although temporal variations in soil formation are out of the scope of this study, ^{210}Pb profiles and AMS ^{14}C dates were used to build age-depth models. These models were used to infer the average accretion rates of the deposits. The concentration profile of ^{210}Pb was determined at every centimeter for the uppermost 30 cm of all cores except for TE.D, CA.S and RO.S-C (see supplementary material), through quantification of ^{210}Po using alpha spectrometry on a PIPS detector (CANBERRA, Mod. PD-450.18 AM) following Sanchez-Cabeza et al. (1998), at the Universitat Autònoma de Barcelona. Furthermore, seagrass macro debris were selected for radiocarbon dating (S1 supplementary material). The materials selected were previously treated to remove soil particles as detailed in Belshe et al., (2019). Radiocarbon analysis was performed by accelerator mass spectrometry using an NEC Pelletron 500 kV AMS (DirectAMS - Accium BioSciences). Radiocarbon ages were corrected for the reservoir effect (Reimer et al., 2013) and the local anomaly (ΔR=2 ± 26 years, Siani et al., 2000). Radiocarbon dates are expressed as calibrated years before present at 2-sigma confidence interval. Age-depth models were elaborated

using the available ages, either ^{210}Pb derived, radiocarbon derived or both, and using the *rbacon* package for R software (Blaauw and Christeny, 2011; R Core Team, 2019). The age at the surface of the core (the sampling year) was included in the models. The models built for each station can be found in supplementary material.

2.4. Statistical analysis

Cores collected manually were compressed as a result of percussion during sampling (0.8-59.9%; Table 2) (Glew et al., 2001). Core length measured at the laboratory was corrected to approximate field length using an exponential function, under the assumption that compaction increases from the bottom to the top of the core (Morton and White, 1997). From now on, all depths are expressed as decompressed ones. OM data were transformed to C_{org} using a calibration curve (Fourqurean et al., 2012a) for each core calculated as a linear relation between OM and C_{org} with the 10 to 12 samples that were analyzed for C_{org} (r^2= 0.96-0.63). To compare cores with different lengths and time spans, accretion rates (mm yr^{-1}) were calculated as the average of the top meter, by dividing 1000 mm by the age at that depth according to the age-depth model. The data matrix was resampled to select samples with data for all the variables. A principal component analysis (PCA) on the correlation matrix was performed in R version 3.4.3 (R Core Team, 2019), package *psych* (Revelle, 2017), using varimax rotation to maximize the variance of the variables in each component. C_{org} data was previously transformed by a logarithmic transformation while grain size distribution data were transformed by center log ratio to avoid spurious correlation typical of compositional data (Aitchison, 1982). The whole data matrix was scaled to mean 0 and 1 standard deviation. All components with eigenvalues > 1 were considered. Given that the clay content was very low in all samples (Table 2), changes of less than 0.5% would have a high loading in the PCA

after scaling the data matrix, although its geochemical significance would be negligible. For this reason, clay was not included in the analysis. The samples from the two cores from Calaburras (CA.S-C and CA.S-CN) were pooled in the same category (CA.S), as they can be considered replicate cores. Correlations between variables and depth used in the discussion have been calculated using the Spearman method (P<0.005) as our variables did not follow a normal distribution and a linear relationship is not always expected in soil data. (QGIS Development Team, 2020)(R Core Team, 2019; Wickham, 2009).

3. Results

Plant macro-debris were identified during sieving along all cores, except for core PA.I, where macro-debris could not be found between 60 and 120 cm. No general downcore trend was found for the debris not for C_{org}, but for AG.I (rho: 0.59, P<0.001), DE.I (rho: 0.42, P<0.001), ME.S (rho: 0.6, P<0.001) and CA.S, (rho: 0.58, P<0.001). However, C_{org} values were always below 10 % of the total weight of the bulk sample (Fig. 3). The predominant inorganic fraction in the cores was FSands and the less abundant fraction was clay, below 1% in all the cores (Table 2). The uppermost layers of BA.S, RO.S-CN and PA.S cores could not be dated by ^{210}Pb because the profile was altered or mixed. Cores PA.I and RO.S-CN were not ^{14}C-dated due to the lack of enough C_{org} rich suitable material. Thus, age-depth models were not obtained for RO.S-CN station and in the dead meadow stations (RO.S-C and CA.S), the estimation of sediment accretion rates was not attempted as erosion was likely to have occurred (Table 2).

According to the age-depth models the lowest accretion rate was recorded in AG.D, 0.42±0.05 mm yr^{-1} (Table 2, Fig. 4), while the core with the highest accretion rate was PA.I, 7.6±3.8 mm yr^{-1} (Table 2, Fig. 4). The most abundant element was Ca with 45% of the total counts, followed by Fe and Cl

(20-10%); Si and Sr (10-5%); Zr, K and Ti (5-1%); Br, Rb, Al, Mn, Pb and Zn (1-0.1%), and Ni (<0.1%), although these figures changed importantly according to the location of the studied core, as well as the nature and mineralogical composition of the soils (S21 to S36, supplementary material). As expected, owing to the main sedimentological features of the cores, MS was highly variable (94 ± 455 SD; S37, supplementary material); C_{org} was 0.02±0.01 g cm^{-3}(Fig. 3) and the predominant grain size was FSand (67±24%), followed by MSand (12±12%), silt (12±9%), CSand (10±13%), and very low clay contents (0.1±0.2%) (S39, supplementary material).

The PCA yielded five components accounting for 70.1 % of the total variance (27.5%, 18.3%, 9.3%, 8%, and 7%, respectively; Table 3). Most cores were well clustered in the PCA scores projections (Fig. 5), indicating that they differed in the weights of the geochemical gradients represented by the components. All variables but MS showed high communalities (> 0.5, Table 3). PC1 clustered Rb, Fe, Zn, K, Ti, Al, Zr, Si, Mn, Silts, and Pb with positive loadings, against C_{org}, Br and MSand with negative loadings (Table 3, Fig. 5). Overall samples from cores BA.S, DE.I, PA.I, AL.S, ME.S, RO.S-CN and TE.S showed positive PC1 scores (Fig. 6), while cores AG.S, AG.I, AG.D, RO.S, RO.S-C, CA.S and TE.D presented negative scores (Fig. 6). PC2 clustered Sr, Cl, Ca, CSand and MSand with positive loadings against FSand, Si and Zr with negative loadings (Table 3, Fig. 5). Samples from AG.D, DE.I, TE.S and TE.D showed positive scores (Fig. 6) and samples from AG.S, AG.I, BA.S, PA.I, RO.S, RO.S-C, AL.S, CA.S, ME.S, and RO.S-CN had negative scores (Fig. 6). PC3 clustered silts, FSands and Si against MSand, CSand and MS (Table 3, Fig. 5), and essentially separated core ME.S, and to a lesser extent CA.S and AG.S, from the other cores (Fig. 6). PC4 clustered Ni and Pb against Mn and Ca (Table 3, Fig. 5) and distinguished CA.S and RO.S-CN from the rest of the cores (Fig. 6). PC5 clustered S, Br and C_{org} (Table 3, Fig. 5). Cores DE.I, RO.S, RO.S-C, AL.S, ME.S and TE.S showed positive PC5 scores (Fig. 6), while cores AG.S, AG.I, AG.D, BA.S, PA.I, CA.S, RO.S-CN and TE.D had negative scores (Fig. 6).

4. Discussion

4.1 Inputs of silty terrestrial material vs organic matter accumulation

High positive loadings in PC1 include elements generally related with silty lithogenic materials (Rb, Fe, Zn, K, Ti, Al, Zr, Si, Mn and Pb) (Rothwell and Croudace, 2015) against C_{org}, Br and MSands, with moderate negative loadings (Table 3). This component is likely indicating inputs of terrestrial silty sediments either from river discharge or runoff of ephemeral streams. Cores with positive scores may thus reflect a higher influence of terrestrial silty material in meadows composition, as it happens in BA.S, DE.I, PA.I, AL.S and ME.S meadows (Fig. 6). Positive PC1 scores can be explained by the interaction of several local factors like the catchment area, the slope and the runoff. BA.S and PA.I are the station with the higher sediment accretion rate, however, DE.I, AL.S and ME.S do not show particularly high accretion values (Table 2). This would reinforce the hypothesis of positive values of PC1 reflecting mineral fluxes from the continental catchments of the meadows. Therefore, specific geological features of the catchment, such as its lithological composition and its degree of fracturation due to tectonic processes, and coastal dynamics (i.e. sediment redistribution) would influence PC1 scores as well.

On the other hand, the covariation between C_{org} and Br was already expected, as Br tends to bind to OM during humification (Leri et al., 2014; Martínez-Cortizas et al., 2016) and it can be used as a proxy for marine OM (e.g. Gribble, 2000; Dembitsky, 2002; Ziegler et al., 2008). This component seems to be reflecting a balance between meadow OM production and silty lithogenic inputs. A similar balance was also found in the elemental composition analysis of a *P. oceanica* meadow soil from the northeast of the Iberian Peninsula (Piñeiro-Juncal et al., 2020). In that soil, OM%, and consequently C_{org}%, was highest at the top and declined downcore in the first 100 cm, following an

exponential curve linked to OM decay observed also by Serrano et al. (2012). However, the C_{org} distribution with soil depth in our data (Fig. 3) does not seem to show this exponential decay curve, as also observed in cores from Florida Bay (USA), Shark Bay (Australia), Mallorca Islands (Spain) or in a collection of *Zostera marina* cores from the Northern hemisphere (Fourqurean et al., 2012b; Mazarrasa et al., 2017; Kindeberg et al., 2019). The C_{org} content is not only the result of how much of the buried C_{org} has been mineralized but also of how much C_{org} was buried in the first place. In stable environments, were C_{org} inputs to the meadow do not change noticeably over time, decay may be expected to be the leading process controlling C_{org} content with soil depth. Moreover, in our analysis the C_{org} content was expressed as C_{org} density (g cm^{-3}), instead of as percentage (%), to allow the comparison of carbon accumulation among cores with different densities. The vertical distribution between the C_{org} expressed in percentage or in density is quite different (Fig. 3), but still, neither distribution fits a decay curve. On the contrary, C_{org} density increased significantly with depth in four of our stations, as found in *Posidonia spp.* cores from Cockburn Sound (Australia) and Cabrera Island (Spain) (Serrano et al., 2016c; Belshe et al., 2019). The increase of C_{org} density with depth in our deposits may be related to the progressive soil compaction of older soil due to accretion. Even when OM mineralization is lowering the OM content in the sample, compaction results in an increase in soil density and a concomitant increase in the amount of carbon per volume unit. If OM degradation and soil compaction were the only processes taking place, C_{org} content would follow a trend with depth, either increasing or decreasing depending on which one predominates. However, this is hardly the case in our data (Fig. 3). Hence, to our best understanding, the vertical fluctuations in soil C_{org} content is probably reflecting temporal variability in OM inputs, which would thus play an important role in C_{org} accumulation in the studied seagrass deposits.

4.2 Grain-size distribution in the soil cores

The second component of the PCA seems to reflect differences in soil texture (Table 3, Fig. 5). Higher Sr and Ca concentrations occur in coarser substrata (positive PC2 loadings) and are probably linked to biogenic carbonates and bioclasts (Croudace and Rothwell, 2015), as seagrasses facilitate bio-precipitation of carbonates (Hendriks et al., 2014). However, along the Andalusian coast there are several outcrops of carbonate rocks (Fig. 1) and the contribution of this continental terrigenous fraction to Ca content cannot be completely discarded. Chlorine has been found to be a water saturation indicator in marine sediments (Hennekam and De Lange, 2012). Soils made up with coarse particles present large porosity and would have a lower water residence time and a higher content of marine water indicators, such as Cl, compared to soils composed by finer particles with higher water resident times, in which the interstitial water would be enriched in compounds derived from chemical reactions in the soil; e.g. OM mineralization or carbonate dissolution (Marbà et al., 2006). On the other hand, Si and Zr showed negative loadings in PC2, indicative of the siliciclastic nature of the fine sandy sediments (see 4.1).

The cores with coarser textures and thus higher porosity, are TE.D, AG.D and DE.I (Table 2). The three cores have been collected below 15 m of water column, farther from the coast than in shallow stations, in relatively open waters. The coarser substrates in these stations could be the result of higher resuspension and export of fine particles (van Katwijk et al., 2010) but the ^{210}Pb profile of AG.D and DE.I did not show any signal of post-depositional disturbances (S6, supplementary material), being resuspension unlikely. Therefore, it is plausible that the bulk of the sediment discharged from inland areas may have been trapped in the shallower meadow areas closest to the shore, those further offshore receiving a much smaller input as *Posidonia oceanica* canopy is known to increase sedimentation, promoting fine fraction deposition (Terrados and Duarte, 2000; Hendriks et al., 2008). When the hydrodynamic force or the sediment load is high

enough to bring sediments to more distal parts of the meadow, the deposit may become enriched in coarser material.

As said before, DE.I core was sampled in a polluted area in which the meadow was in an advanced state of degradation (Marbà et al., 2015; Consejería de Agricultura Ganadería Pesca y Desarrollo Sostenible, 2017). Field observations during sampling also indicated that there was a very soft substrate, confirmed by an anomalously low density in the upper parts of the core. This has been interpreted as the effect of the chemical degradation of the OM deposited that implied an increased porosity and, consequently a decreased density. However, increasing shoot mortality is likely to have an impact over the rhizosphere, but not over deeper sections of the soil (Piñeiro-Juncal et al., 2020a). DE.I showed high PC2 scores along the core and not only in the upper part (S41, supplementary material), but OM degradation promoted by the demise in plant cover, is not likely to be the sole explanation. As no other core was sampled in this location we cannot ascertain if there is a change in texture between the shallower and the deeper part of the meadow as found for TE.D and AG.D. The shallow meadow in front of Deretil has completely disappeared in a coastal extension of more than 2 km (Moreno et al., 1999). Nevertheless, this loss is relatively recent (in the last 5 decades), and thus would not have affected the processes that formed the soil in the last 3620 cal. yr BP (Table 2), the time encompassed by the DE.I core.

Two of the *C. nodosa* cores, BA.S and PA.I, are the ones presenting the lowest PC2 scores, the largest content of FSands (Fig. 5 and 6), the lowest content of MSand (0 for both cores) and CSand (<1% for both cores) and the highest accretion rates (BA.S 4.4±1.1 mm yr^{-1}, PA.I 7.6±3.8 mm yr^{-1}; Fig. 4; Table 2). *Cymodocea nodosa* is known to be a pioneer species, earlier colonizer of areas that could be later colonized by larger species, as *P. oceanica* (Molinier and Picard, 1952). However, the *C. nodosa* meadow at BA.S has existed for at least some hundreds of years (BAS 355 cal. yr BP at the bottom of the core; Table 2), as *C. nodosa* macro debris could be found along the whole core,

with no remains of *P. oceanica*. Although no assurance can be provided that the PA.I meadow was stable over the time covered by this soil record, as there were no traces of *C. nodosa* macro debris between 60 and 120 cm deep, *P. oceanica* debris were also absent in that section as well. This may be due to the unsuitability of the environment for the colonization of larger seagrass species. *Posidonia oceanica* has been found to grow from fine sandy to rocky bottoms, but not on muddy ones (i.e. silt+clay, Mazzella et al., 1993, Bellan-Santini et al., 1994; De Falco et al., 2006; Gobert et al., 2006). Although silt have a low loading in this component, it is possible that a high content in FSand with almost no MSand or CSand content would negatively affect *P. oceanica* performance. Furthermore, punctual sediment burial of the leaves beyond 5 cm triggers a decline in the shoot population of well-developed *P. oceanica* meadows (Manzanera et al., 2011; Gera et al., 2014), while *C. nodosa* seedlings have been found to tolerate up to 7 cm of punctual burial and its vertical growth is promoted by < 4 cm of punctual burial (Marbà and Duarte, 1994). Therefore, *C. nodosa* would be more suited for high accretion environments than *P. oceanica*. Although our accretion rates are lower, two conditions need to be considered. First, the accretion rates are averages of the top meter, where soil compaction is very likely to have already occurred, and may be underestimating punctual sedimentation rates. Second, the studies cited are experiments of punctual burial while our accretion rates integrate long term burial. It is possible that the maintained burial stress of stations PA.I and BA.S (the highest of our stations) may have further diminished *P. oceanica* performance, preventing the establishment of a meadow. The AG.I station showed similar accretion rates to BA.S, but a much coarser sediment and ME.S showed a high content of fine sediments but a much lower accretion rate and both areas host a *P. oceanica* meadow. This suggests that both factors, grain size and high accretion rates, are playing a synergic role in the exclusion of *P. oceanica* from the area.

4.3 High energy transport of coarse material

The third component clustered CSand and MSand with MS, with negative loadings, against silt, with positive loading (Table 3, Fig. 5). The high anti-covariation between silts and MS (0.67 and -0.62 loadings respectively, Table 2) indicates that minerals with higher MS were probably linked to medium and coarse materials. MS in seagrass deposits has been related to influxes of magnetic particles eroded from catchment topsoils and incorporated into marine sediments and seagrasses soils, due to changes in land use or flooding events (López-Merino et al., 2017). The possibility of PC3 being the signal of flooding episodes seems to be reinforced by the association between the MS and coarse grain-sized particles in our cores, as the arrival of larger particles is related to high energy transport (van Rijn, 1993). This component would be interpreted as the signal of coarse material discharges, contrary to PC1 that relates to the continuous silty inputs - transported in low energy environments - and its balance with OM accumulation in the meadows. The most outstanding core in PC3 scores is ME.S (Fig. 6), with the lowest scores. Core ME.S was sampled near a steep slope coastal area (Instituto de Cartografía de Andalucia, 2007) that could have promoted high energy runoff. The distribution of PC3 scores in ME.S shows a sharp decrease at 25-30 cm (S42, supplementary material), pointing towards a punctual event of coarse material discharge as the main source of its low PC3 values. Other two cores show low PC3 scores, CA.S and the upper part of AG.S core (S42, supplementary material). Scores in CA.S are quite stable along the core (S42, supplementary material), which can be implying that the sedimentary particles arriving to the meadow were always generated in a high-energy environment. On the other hand, scores from AG.S are low between 25 and 50 cm and again between 100 and 140 cm (S42, supplementary material), suggesting the alternation between phases of high and low energy sediment transport.

4.4 Metals bind to organic matter

The fourth component of the PCA clusters Ni, Pb and Br against Ca and Mn (Table 3). The association of Ni and Pb with Br could be indicating the bonding of metals and halogens to humified OM (Leri et al., 2014; Martínez-Cortizas et al., 2016). Furthermore, Pb has been found to be selectively preserved during the degradation of seagrass tissues (Lyngby and Brix, 1989). The low loading of C_{org} in this component could be indicating that not all OM but only humified OM is active in metal binding. However, in a *P. oceanica* meadow from the northeast of the Iberian peninsula (Portlligat, Spain) a positive covariation with the fine OM fraction (<2 mm) was found, but not with the humified OM (inferred by the covariance of S, P, Br and Cl; Piñeiro-Juncal et al., 2020). A specific study would be needed to clarify the behavior of metals in seagrass deposits. As found in our study, the core of the Portlligat meadow also showed a negative relationship between Pb and Ca (also to $CaCO_3$) concentrations. This correlation was interpreted as a negative effect of Pb over bio-calcifying organisms or as relative dilution effect between OM and carbonates, as Pb was associated with OM (Piñeiro-Juncal et al., 2020). However, this correlation can also be an indication of a positive relationship between heavy metals content and fine particles, previously observed in other marine areas (e.g., Dang et al., 2015; Yao et al., 2015; Remeikaitė-Nikienė et al., 2018), as $CaCO_3$ is often found in the form of coarse particles.

4.5. Humified organic matter

The main variables associated with the fifth component of the PCA were S and Br, and a moderate loading of C_{org} (Table 3, Fig. 5). Both Br and S are proxies for OM (Rothwell and Croudace, 2015). As stated before, the first one bonds to OM during humification (Leri et al., 2014; Martínez-Cortizas et al., 2016). This balance has been already detected in an XRF analysis in the core of Portlligat mentioned above (Piñeiro-Juncal et al., 2020b). Cores with higher loadings in PC5 were all the shallow *P. oceanica* cores, except CA.S (Fig. 6). While *C. nodosa* cores showed values similar to

those of deeper *P. oceanica* meadows. *Posidonia oceanica* carbon stock has been found to be maximum at shallow waters, linked to higher light penetration and primary production (Serrano et al., 2014). *Cymodocea nodosa* has a lower primary production than *P. oceanica* and accumulates far less carbon in its soils (Luque and González, 2004), resulting in much lower C_{org} average content in our cores (0.025±0.010 vs 0.002±0.001 C_{org} g cm^{-3}), that would necessarily derive in less humified OM. The station with the lowest scores in this component was CA.S, despite being a shallow *P. oceanica* meadow. CA.S together with RO.S-C, is one of the two dead *P. oceanica* meadows sampled in this study. Despite of this, RO.S-C showed one of the highest values in PC5. The lack of accumulation or faster degradation and wash of the humified OM in the mat could be related to specific impacts derived from the loss of the canopy in dead meadows, from differences in the time elapsed since the loss, or to intrinsic physico-chemical traits of the soil. A specific study would be necessary to explore these possible factors, which are of great interest to model carbon stocks loss after blue carbon habitat degradation.

5. Conclusions

In this study we found five geochemical signals that could be linked to seagrass soil formation processes: (1) accumulation of terrestrial silty material, balanced with OM accumulation; (2) soil grain size changes, which might be affected by the orientation and distance from the discharging point of sediments, and by local hydrodynamism; (3) coarse sediments discharge, that we related to high energy transport; (4) the accumulation of metal-OM compounds (and negative correlation with carbonate), by mechanisms that need further research; and, finally, (5) OM bromination, linked to OM degradation within the soil. The first three processes are related to the continental catchment that furnishes the meadows with terrigenous materials. Together, they explain 55% of

the total variance of our data, revealing the determinant terrestrial influence over these marine coastal ecosystems, working as a juncture between land and sea. Thus, land use management affects the amount and quality of sediments reaching the sea, which in turn, have an impact in seagrass soil composition. As discussed for PC2, sediment grain size and amount may play a central role in controlling species colonization along the Mediterranean coast. Knowledge about environmental conditions promoting the establishment of a given seagrass species would help to understand the causes for meadow deterioration and to develop more efficient restoration projects. Here we show that the study of current and past conditions of stable monospecific meadows can shed light on this question. In our cores, C_{org} depth distribution did not follow any particular trend, pointing to temporal changes in OM inputs to the meadow as an influential factor in its accumulation. Finally, our results on metal-OM bonding, in line with those found in a previous study, suggest the need of specific research to clarify metal's behavior in seagrass beds and the potential relation between Pb deposition and carbonates accumulation.

6. Acknowledgments

This research was funded by the LIFE BLUE NATURA project (LIFE14CCM/ES/000957). Carmen Leiva-Dueñas was supported by a PhD scholarship funded by the Spanish Ministry of Science, Innovation and Universities (FPU15/01934). This is a paper of the Group of Benthic Ecology 2014 SGR 120 in collaboration with the 2017 SGR 1588. We thank the Marine technicians Jose Miguel Remón, Agustín Barrajón and Diego Moreno, from the Andalusian Environmental Service, AMAyA, for sharing with us their thorough knowledge about the recent environmental History of the sites studied here.

7. Bibliography

Agawin, N.S.R., Duarte, C.M., 2002. Evidence of direct particle trapping by a tropical seagrass meadow. Estuaries 25, 1205–1209. https://doi.org/10.1007/BF02692217

Aitchison, J., 1982. The statistical analysis of compositional data. J. R. Stat. Soc. Ser. B 44, 139–177.

Alcoverro, T., Romero, J., Duarte., C.M., Lopez, N.I., 1997. Spatial and temporal variations in nutrient limitation of seagrass *Posidonia oceanica* growth in the NW Mediterranean. Mar. Ecol. Prog. Ser. 146, 155–161. https://doi.org/10.5301/jn.5000098

Bellan-Santini, D., Lacaze, J.-C., Poizat, C., Pérès, J.-M., 1994. Les biocénoses marines et littorales de Méditerranée, synthèse, menaces et perspectives. Collect. patrimoines Nat.

Belshe, E.F., Sanjuan, J., Leiva-Dueñas, C., Piñeiro-Juncal, N., Serrano, O., Lavery, P.S., Mateo, M.A., Leiva-Dueñas, C., Piñeiro-Juncal, N., Serrano, O., Lavery, P.S., Mateo, M.A., 2019. Modeling organic carbon accumulation rates and residence times in coastal vegetated ecosystems. J. Geophys. Res. Biogeosciences 124, 3652–3671. https://doi.org/10.1029/2019jg005233

Blaauw, M., Christeny, J.A., 2011. Flexible paleoclimate age-depth models using an autoregressive gamma process. Bayesian Anal. 6, 457–474. https://doi.org/10.1214/11-BA618

Borum, J., Sand-jensen, K., Binzer, T., Pedersen, O., Greve, T.M., 2006. Oxygen movement in seagrasses, in: Seagrasses: Biology, Ecology and Conservation. Springer, pp. 255–270.

Boudouresque, C., Meinesz, A., 1982. Découverte de l´herbier de posidonie.

CAGPDS (Consejería de Agricultura Ganadería Pesca y Desarrollo Sostenible), 2014. Evolución de los grupos climáticos actualizados al 4o Informe del IPCC [WWW Document]. URL http://www.juntadeandalucia.es/medioambiente/site/portalweb/menuitem.7e1cf46ddf59bb227a9ebe205510e1ca/?vgnextoid=

40615abf281b4410VgnVCM2000000624e50aRCRD&vgnextchannel=
9970c4f9d8a26310VgnVCM2000000624e50aRCRD#apartado3a5478983e2f6610Vg-
nVCM100000341de (accessed 10.22.19).

Cebrián, J., Pedersen, M.F., Kroeger, K.D., Valiela, I., 2000. Fate of production of the seagrass *Cymodocea nodosa* in different stages of meadow formation. Mar. Ecol. Prog. Ser. 204, 119–130. https://doi.org/10.3354/meps204119

Consejería de Agricultura Ganadería Pesca y Desarrollo Sostenible, 2017. Informe regional programa de gestion del medio marino andaluz.

Croudace, I.W., Rothwell, R.G., 2015. Micro-XRF studies of sediment cores. Applications of a non-destructive tool for the environmental sciences, Springer. https://doi.org/10.1515/logos-2016-0008

Dang, D.H., Lenoble, V., Durrieu, G., Omanović, D., Mullot, J.U., Mounier, S., Garnier, C., 2015. Seasonal variations of coastal sedimentary trace metals cycling: Insight on the effect of manganese and iron (oxy)hydroxides, sulphide and organic matter. Mar. Pollut. Bull. 92, 113–124. https://doi.org/10.1016/j.marpolbul.2014.12.048

De Falco, G., Baroli, M., Murru, E., Piergallini, G., Cancemi, G., 2006. Sediment analysis evidences two different depositional phenomena influencing seagrass distribution in the Gulf of Oristano (Sardinia, Western Mediterranean). J. Coast. Res. 225, 1043–1050. https://doi.org/10.2112/00129.1

Demas, G.P., Rabenhorst, M.C., 2001. Factors of subaqueous soil formation: A system of quantitative pedology for submersed environments. Geoderma 102, 189–204. https://doi.org/10.1016/S0016-7061(00)00111-7

Dembitsky, V.M., 2002. Bromo- and iodo-containing alkaloids from marine microorganisms and sponges. Russ. J. Bioorganic Chem. 28, 170–182.

Duarte, C.M., 1991. Seagrass depth limits. Aquat. Bot. 40, 363–377. https://doi.org/10.1016/0304-3770(91)90081-F

Duarte, C.M., Holmer, M., Marbà, N., 2005a. Plant-microbe interactions in seagrass meadows, in: Interactions Between Macro- and Microorganisms in Marine Sediments. pp. 31–60.

Duarte, C.M., Middelburg, J.J., Caraco, N., 2005b. Major role of marine vegetation on the oceanic carbon cycle. Biogeosciences 2, 1–8. https://doi.org/10.5194/bgd-1-659-2004

Fernandes, M., Bryars, S., Mount, G., Miller, D., 2009. Seagrasses as a sink for wastewater nitrogen: The case of the Adelaide metropolitan coast. Mar. Pollut. Bull. 58, 303–308. https://doi.org/10.1016/j.marpolbul.2008.10.006

Fourqurean, J.W., Duarte, C.M., Kennedy, H., Marbà, N., Holmer, M., Mateo, M.A., Apostolaki, E.T., Kendrick, G.A., Krause-Jensen, D., McGlathery, K.J., Serrano, O., 2012a. Seagrass ecosystems as a globally significant carbon stock. Nat. Geosci. 5, 505–509. https://doi.org/10.1038/ngeo1477

Fourqurean, J.W., Kendrick, G.A., Collins, L.S., Chambers, R.M., Vanderklift, M.A., 2012b. Carbon, nitrogen and phosphorus storage in subtropical seagrass meadows: Examples from Florida Bay and Shark Bay. Mar. Freshw. Res. 63, 967–983. https://doi.org/10.1071/MF12101

Gacia, E., Duarte, C.M., 2001. Sediment retention by a Mediterranean *Posidonia oceanica* meadow: The balance between deposition and resuspension. Estuar. Coast. Shelf Sci. 52, 505–514. https://doi.org/DOI: 10.1006/ecss.2000.0753

Gera, A., Pagès, J.F., Arthur, R., Farina, S., Roca, G., Romero, J., Alcoverro, T., 2014. The effect of a

centenary storm on the long-lived seagrass *Posidonia oceanica*. Limnol. Oceanogr. 59, 1910–1918. https://doi.org/10.4319/lo.2014.59.6.1910

Glew, J., Smol, J., Last, W., 2001. Sediment core collection and extrusion, in: Tracking Environmental Change Using Lake Sediments. pp. 73–105. https://doi.org/10.1007/0-306-47669-X_5

Gobert, S., Cambridge, M.L., Velimirov, B., Pergent, G., Lepoint, G., Bouquegneau, J.-M., Dauby, P., Pergent-Martini, C., Walker, D.I., 2006. Biology of *Posidonia*, in: Seagrasses: Biology, Ecology and Conservation. pp. 387–408. https://doi.org/10.1007/978-1-4020-2983-7_17

Gribble, G.W., 2000. The natural production of organobromine compounds. Environ. Sci. Pollut. Res. 7, 37–49.

Gruber, R.K., Kemp, W.M., 2010. Feedback effects in a coastal canopy-forming submersed plant bed. Limnol. Oceanogr. 55, 2285–2298. https://doi.org/10.4319/lo.2010.55.6.2285

Hansen, J.C.R., Reidenbach, M.A., 2012. Wave and tidally driven flows in eelgrass beds and their effect on sediment suspension. Mar. Ecol. Prog. Ser. 448, 271–287. https://doi.org/10.3354/meps09225

Hartog, C. Den, Kuo, J., 2006. Taxonomy and biogeography of seagrasses, in: Seagrasses: Biology, Ecology and Conservation. pp. 1–23. https://doi.org/10.1007/978-1-4020-2983-7_1

Hendriks, I.E., Bouma, T.J., Morris, E.P., Duarte, C.M., 2010. Effects of seagrasses and algae of the Caulerpa family on hydrodynamics and particle-trapping rates. Mar. Biol. 157, 473–481. https://doi.org/10.1007/s00227-009-1333-8

Hendriks, I.E., Olsen, Y.S., Ramajo, L., Basso, L., Moore, T.S., Howard, J., Duarte, C.M., Steckbauer, A., Moore, T.S., Howard, J., Duarte, C.M., 2014. Photosynthetic activity buffers ocean

acidification in seagrass meadows. Biogeosciences 11, 333–346. https://doi.org/10.5194/bg-11-333-2014

Hendriks, I.E., Sintes, T., Bouma, T.J., Duarte, C.M., 2008. Experimental assessment and modeling evaluation of the effects of the seagrass *Posidonia oceanica* on flow and particle trapping. Mar. Ecol. Prog. Ser. 356, 163–173. https://doi.org/10.3354/meps07316

Hennekam, R., De Lange, G., 2012. X-ray fluorescence core scanning of wet marine sediments: Methods to improve quality and reproducibility of highresolution paleoenvironmental records. Limnol. Oceanogr. Methods 10, 991–1003. https://doi.org/10.4319/lom.2012.10.991

Holmer, M., 2018. Productivity and biogeochemical cycling in seagrass ecosystems, in: Coastal Wetlands: An Integrated Ecosystem Approach. Elsevier B.V., pp. 443–477. https://doi.org/10.1016/B978-0-444-63893-9.00013-7

Instituto de Cartografía de Andalucia, 2007. Mapa informacion geografica de Andalucia.

Instituto Geológico y Minero de España, 1995. Mapa Geológico de la Península Ibérica, Baleares y Canarias a escala 1:1.000.000.

Jensen, S.I., Kühl, M., Priemé, A., 2007. Different bacterial communities associated with the roots and bulk sediment of the seagrass *Zostera marina*. FEMS Microbiol. Ecol. 62, 108–117. https://doi.org/10.1111/j.1574-6941.2007.00373.x

Kaal, J., Serrano, O., Nierop, K.G.J., Schellekens, J., Martínez Cortizas, A., Mateo, M.-Á., 2016. Molecular composition of plant parts and sediment organic matter in a Mediterranean seagrass (*Posidonia oceanica*) mat. Aquat. Bot. 133, 50–61. https://doi.org/10.1016/j.aquabot.2016.05.009

Kennedy, H., Gacia, E., Kennedy, D.P., Papadimitriou, S., Duarte, C.M., 2004. Organic carbon sources to SE Asian coastal sediments. Estuar. Coast. Shelf Sci. 60, 59–68. https://doi.org/10.1016/j.ecss.2003.11.019

Kindeberg, T., Röhr, E., Moksnes, P.O., Boström, C., Holmer, M., 2019. Variation of carbon contents in eelgrass (Zostera marina) sediments implied from depth profiles. Biol. Lett. 15. https://doi.org/10.1098/rsbl.2018.0831

Koch, E.W., 2001. Beyond light: Physical, geological, and geochemical parameters as possible submersed aquatic vegetation habitat requirements. Estuaries 24, 1–17. https://doi.org/10.1007/BF02693942

Lavery, P.S., Mateo, M.Á., Serrano, O., Rozaimi, M., 2013. Variability in the carbon storage of seagrass habitats and its implications for global estimates of Blue Carbon ecosystem service. PLoS One 8, 1–12. https://doi.org/10.1371/journal.pone.0073748

Leiva-Dueñas, C., Martínez Cortizas, A., Pineiro-Juncal, N., Díaz-Almela, E., Garcia-Orellana, J., Mateo, M.A., 2021. Long-term dynamics of production in western Mediterranean seagrass meadows: Trade-offs and legacies of past disturbances. Sci. Total Environ. 754, 142117. https://doi.org/10.1016/j.scitotenv.2020.142117

Leri, A.C., Mayer, L.M., Thornton, K.R., Ravel, B., 2014. Bromination of marine particulate organic matter through oxidative mechanisms. Geochim. Cosmochim. Acta 142, 53–63. https://doi.org/10.1016/j.gca.2014.08.012

López-Merino, L., Colás-Ruiz, N.R., Adame, M.F., Serrano, O., Martínez Cortizas, A., Mateo, M.A., 2017. A six thousand-year record of climate and land-use change from Mediterranean seagrass mats. J. Ecol. 1–12. https://doi.org/10.1111/1365-2745.12741

Luque, Á.A., González, J.T., 2004. Praderas y bosques marinos de Andalucía.

Lyngby, J.E., Brix, H., 1989. Heavy metals in eelgrass (Zostera marina L.) during growth and decomposition. Hydrobiologia 176–177, 189–196. https://doi.org/10.1007/BF00026554

Manzanera, M., Alcoverro, T., Tomas, F., Romero, J., 2011. Response of *Posidonia oceanica* to burial dynamics. Mar. Ecol. Prog. Ser. 423, 47–56. https://doi.org/10.3354/meps08970

Marbà, N., Álvarez, E., Vivas, M.S., Barrajón, A., Moreno, D., Remón, J.M., De la Rosa, J., Leon, D., Peñalver, P., Diaz-Almela, E., Mendoza, R.M., 2015. Estudio demografico de *Posidonia oceanica*. Proyecto LIFE09NAT/ES/000534, Instituto Mediterraneo de Estudios Avanzados.

Marbà, N., Duarte, C.M., 1994. Growth response of the seagrass Cymodocea nodosa to experimental burial and erosion. Mar. Ecol. Prog. Ser. 107, 307. https://doi.org/10.3354/meps107307

Marbà, N., Holmer, M., Gacia, E., Barrón, C., 2006. Seagrass beds and coastal biogeochemistry, in: Seagrasses: Biology, Ecology and Conservation. pp. 133–155.

Martínez-Cortizas, A., Ferro-Vázquez, C., Kaal, J., Biester, H., Casais, M.C., Rodríguez, T.T., Lado, L.R., Martinez Cortizas, A., Ferro-Vázquez, C., Kaal, J., Biester, H., Costa Casais, M., Taboada Rodríguez, T., Rodríguez-Lado, L., 2016. Bromine accumulation in acidic black colluvial soils. Geochim. Cosmochim. Acta 174, 143–155. https://doi.org/10.1016/j.gca.2015.11.013

Mateo, M.A., Cebrián, J., Dunton, K., Mutchler, T., 2006. Carbon flux in seagrass ecosystems, in: Seagrasses: Biology, Ecology and Conservation. pp. 159–192. https://doi.org/10.1007/978-1-4020-2983-7_7

Mateo, M.A., Renom, P., Michener, R.H., 2010. Long-term stability in the production of a NW Mediterranean *Posidonia oceanica* (L.) Delile meadow. Palaeogeogr. Palaeoclimatol.

Palaeoecol. 291, 286–296. https://doi.org/10.1016/j.palaeo.2010.03.001

Mateo, M.A., Romero, J., Pérez, M., Littler, M.M., Littler, D.S., 1997. Dynamics of millenary organic deposits resulting from the growth of the Mediterranean seagrass *Posidonia oceanica*. Estuar. Coast. Shelf Sci. 44, 103–110. https://doi.org/10.1006/ecss.1996.0116

Mazarrasa, I., Marbà, N., Garcia-Orellana, J., Masqué, P., Arias-Ortiz, A., Duarte, C.M., 2017. Effect of environmental factors (wave exposure and depth) and anthropogenic pressure in the C sink capacity of *Posidonia oceanica* meadows. Limnol. Oceanogr. 62, 1436–1450. https://doi.org/10.1002/lno.10510

Mazarrasa, I., Marbà, N., Lovelock, C.E., Serrano, O., Lavery, P.S., Fourqurean, J.W., Kennedy, H., Mateo, M.A., Krause-Jensen, D., Steven, A.D.L., Duarte, C.M., 2015. Seagrass meadows as a globally significant carbonate reservoir. Biogeosciences 12, 4993–5003. https://doi.org/10.5194/bg-12-4993-2015

Mazzella, L., Scipione, M.B., Gambi, M.C., Buia, M.C., Lorenti, M., Zupo, V., Cancemi, G., 1993. The Mediterranean seagrass Posidonia oceanica and Cymodocea nodosa. A comparative overview, in: First International Conference on the Mediterranean Coastal Environment, MEDCOAST. pp. 103–116.

Molinier, R., Picard, J., 1952. Recherches sur les herbiers de Phanérogames marines du littoral méditerranéen français. Masson.

Moreno, D., Aguilera, P. a., Castro, H., 2001. Assessment of the conservation status of seagrass (Posidonia oceanica) meadows: implications for monitoring strategy and the decision-making process. Biol. Conserv. 102, 325–332. https://doi.org/10.1016/S0006-3207(01)00080-5

Moreno, D., Aguilera, P.A., Castro, H., Martínez Vidal, J.L., Martínez Sola, F., Sanz, F., 1999.

Valoración del impacto de los vertidos hídricos industriales en el litoral: aproximación metodológica al estudio de la pradera de Posidonia oceanica (L.) Delile, in: Minería, Industria y Medio Ambiente En Al Cuenca Mediterránea. Universidad de Almería, p. 464.

Moreno, D., Guirado, J., 2003. Nuevos datos sobre la distribución de las fanerogamas marinas en las provincias de Almería y Granada (SE España). Acta Bot. Malacit. 28, 105. https://doi.org/10.24310/abm.v28i0.7270

Morton, R.A., White, W.A., 1997. Characteristics of and corrections for core shortening in unconsolidated sediments. J. Coast. Res. 13, 761–769.

Nellemann, C., Corcoran, E., Duarte, C.M., Valdés, L., De Young, C., Fonseca, L., Grimsditch, G., 2009. Blue carbon: the role of healthy oceans in binding carbon: a rapid response assessment.

Piñeiro-Juncal, N., Kaal, J., Cezar Fornazier Moreira, J., Martínez Cortizas, A., Rodrigues Lambais, M., Luis Otero, X., Ángel Mateo, M., 2020a. Cover loss in a seagrass Posidonia oceanica meadow accelerates soil organic matter turnover and alters soil prokaryotic communities. Org. Geochem. 104–140. https://doi.org/https://doi.org/10.1016/j.orggeochem.2020.104140

Piñeiro-Juncal, N., Leiva-Dueñas, C., Serrano, O., Mateo, M.Á., Martínez-Cortizas, A., 2020b. Pedogenic processes in a *Posidonia oceanica* mat. Soil Syst. 4, 1–15. https://doi.org/10.3390/soilsystems4020018

QGIS Development Team, 2020. QGIS Geographic Information System.

R Core Team, 2019. R: A language and environment for statistical computing.

Red de Información Ambiental de Andalucia, 2020. Lithological map of Andalusia [WWW

Document]. Map. URL http://www.juntadeandalucia.es/medioambiente/site/rediam/menuitem.04dc44281e5d53cf8ca78ca731525ea0/?vgnextoid=6a7b9859ccb0a210VgnVCM2000000624e50aRCRD&vgnextchannel=36faa7215670f210VgnVCM1000001325e50aRCRD&vgnextfmt=rediam&lr=lang_es (accessed 4.28.20).

Reimer, P.J., Bard, E., Bayliss, A., Beck, J.W., Blackwell, P.G., Ramsey, C.B., Buck, C.E., Cheng, H., Edwards, R.L., Friedrich, M., Grootes, P.M., Guilderson, T.P., Haflidason, H., Hajdas, I., Hatté, C., Heaton, T.J., Hoffmann, D.L., Hogg, A.G., Hughen, K.A., Kaiser, K.F., Kromer, B., Manning, S.W., Niu, M., Reimer, R.W., Richards, D.A., Scott, E.M., Southon, J.R., Staff, R.A., Turney, C.S.M., van der Plicht, J., 2013. IntCal13 and Marine13 Radiocarbon Age Calibration Curves 0–50,000 Years cal BP. Radiocarbon 55, 1869–1887. https://doi.org/DOI: 10.2458/azu_js_rc.55.16947

Remeikaitė-Nikienė, N., Garnaga-Budrė, G., Lujanienė, G., Jokšas, K., Stankevičius, A., Malejevas, V., Barisevičiūtė, R., 2018. Distribution of metals and extent of contamination in sediments from the south-eastern Baltic Sea (Lithuanian zone). Oceanologia 60, 193–206. https://doi.org/10.1016/j.oceano.2017.11.001

Revelle, W., 2017. psych: procedures for personality and psychological research.

Romero, J., Pérez, M., Mateo, M.A., Sala, E., 1994. The belowground organs of the Mediterranean seagrass *Posidonia oceanica* as a biogeochemical sink. Aquat. Bot. 47, 13–19. https://doi.org/10.1016/0304-3770(94)90044-2

Rothwell, R.G., Croudace, I.W., 2015. Twenty years of XRF core scanning marine sediments: what do geochemical proxies tell us?, in: Micro-XRF Studies of Sediment Cores: Applications of a Non-Destructive Tool for the Environmental Sciences. pp. 25–102.

Rueda, J.L., Salas, C., Marina, P., 2008. Seasonal variation in a deep subtidal *Zostera marina* L. bed in southern Spain (western Mediterranean Sea). Bot. Mar. 51, 92–102. https://doi.org/10.1515/BOT.2008.016

Sanchez-Cabeza, J.A., Masqué, P., Ani-Ragolta, I., 1998. 210Pb and 210Pb analysis in sediments and soils by microwave acid digestion. J. Radioanal. Nucl. Chem. 227, 19–22.

Serrano, O., Davis, G., Lavery, P.S., Duarte, C.M., Martinez-Cortizas, A., Mateo, M.A., Masqué, P., Arias-Ortiz, A., Rozaimi, M., Kendrick, G.A., 2016a. Reconstruction of centennial-scale fluxes of chemical elements in the Australian coastal environment using seagrass archives. Sci. Total Environ. 541, 883–894. https://doi.org/10.1016/j.scitotenv.2015.09.017

Serrano, O., Lavery, P.S., López-Merino, L., Ballesteros, E., Mateo, M.A., 2016b. Location and associated carbon storage of erosional escarpments of seagrass *Posidonia* mats. Front. Mar. Sci. 3, 1–7. https://doi.org/10.3389/fmars.2016.00042

Serrano, O., Lavery, P.S., Rozaimi, M., Mateo, M.M.Á., 2014. Influence of water depth on the carbon sequestration capacity of seagrasses. Global Biogeochem. Cycles 28, 950–961. https://doi.org/10.1002/2014GB004872.Received

Serrano, O., Mateo, M. a., Renom, P., Julià, R., 2012. Characterization of soils beneath a *Posidonia oceanica* meadow. Geoderma 185–186, 26–36. https://doi.org/10.1016/j.geoderma.2012.03.020

Serrano, O., Mateo, M., Dueñas-Bohórquez, A., Renom, P., López-Sáez, J. a, Martínez Cortizas, A., 2011. The *Posidonia oceanica* marine sedimentary record: A Holocene archive of heavy metal pollution. Sci. Total Environ. 409, 4831–40. https://doi.org/10.1016/j.scitotenv.2011.08.001

Serrano, O., Ricart, A.M., Lavery, P.S., Mateo, M.-A.A., Arias-Ortiz, A., Masque, P., Steven, A.,

Duarte, C.M., Rozaimi, M., Steven, A., Duarte, C.M., 2016c. Key biogeochemical factors affecting soil carbon storage in *Posidonia* meadows. Biogeosciences 13, 4581–4594. https://doi.org/10.5194/bg-13-4581-2016

Siani, G., Paterne, M., Arnold, M., Bard, E., Métivier, B., Tisnerat, N., Bassinot, F., 2000. Radiocarbon reservo ir ages in the mediterranean sea and black sea. Radiocarbon 42, 271–280.

Smit, A.J., Brearley, A., Hyndes, G.A., Lavery, P.S., Walker, D.I., 2005. Carbon and nitrogen stable isotope analysis of an Amphibolis griffithii seagrass bed. Estuar. Coast. Shelf Sci. 65, 545–556. https://doi.org/10.1016/j.ecss.2005.07.002

Terrados, J., Duarte, C.M., 2000. Experimental evidence of reduced particle resuspension within a seagrass (*Posidonia oceanica L.*) meadow. J. Exp. Mar. Bio. Ecol. 243, 45–53. https://doi.org/Doi 10.1016/S0022-0981(99)00110-0

Thomson, A.C.G., Trevathan-Tackett, S.M., Maher, D.T., Ralph, P.J., Macreadie, P.I., 2019. Bioturbator-stimulated loss of seagrass sediment carbon stocks. Limnol. Oceanogr. 64, 342–356. https://doi.org/10.1002/lno.11044

University of Maryland Center for Environmental Science (UMCES), n.d. Integration and Application Network (IAN).

van Katwijk, M.M., Bos, A.R., Hermus, D.C.R., Suykerbuyk, W., 2010. Sediment modification by seagrass beds: Muddification and sandification induced by plant cover and environmental conditions. Estuar. Coast. Shelf Sci. 89, 175–181. https://doi.org/10.1016/j.ecss.2010.06.008

van Rijn, L.C., 1993. Fluid and sediment properties, in: Principles of Sediment Transport in Rivers, Estuaries and Coastal Seas.

Wickham, H., 2009. ggplot2: Elegant Graphics for Data Analysis.

Yao, Q., Wang, X., Jian, H., Chen, H., Yu, Z., 2015. Characterization of the particle size fraction associated with heavy metals in suspended sediments of the yellow river. Int. J. Environ. Res. Public Health 12, 6725–6744. https://doi.org/10.3390/ijerph120606725

Ziegler, M., Jilbert, T., De Lange, G.J., Lourens, L.J., Reichart, G.J., 2008. Bromine counts from XRF scanning as an estimate of the marine organic carbon content of sediment cores. Geochemistry, Geophys. Geosystems 9, 1–6. https://doi.org/10.1029/2007GC001932

Journal Pre-proof

Figures:

Figure 1: Localities sampled and the lithology of their catchments obtained from the Geological Map of the Iberian Peninsula, Baleares and Canarias, 1:1.000.000 (Instituto Geológico y Minero de España, 1995). This figure was built using QGIS software (QGIS Development Team, 2020).

Figure 2: Images of the cores studied. Seagrass symbols from the Integration and Application Network (University of Maryland Center for Environmental Science,;UMCES)

Figure 3: Distribution of C_{org} in each core expressed as carbon density (solid line, g/cm^3) and carbon percentage (dashed line). This figure was built using package *ggplot2* for R software (Wickham, 2009; R Core Team, 2019).

Figure 4: Average of the uppermost meter accretion rate per station (mm yr^{-1}) and its standard error (propagated from the age-depth model).

Figure 5: Biplots of the variables studied in the PCA. A, PC1 vs PC2; B, PC3 vs PC4; C, PC1 vs PC5. The arrows in the left panels indicate the loading of each of the variables for each component. Dots in the right panel indicate the score of each sample grouped by station (colors). The shape of the dots indicates at which water depth the meadow was sampled, D: Deep (18-19 m), I: intermediate (10-16 m), S: Shallow (2.5-7 m). This figure was built using package *ggplot2* for R software (Wickham, 2009; R Core Team, 2019).

Figure 6: Tukey boxplot of PCA scores per station. For each station the solid line indicates the median of the scores; the box indicates the interquartile range; the hanging bars indicate the range excluding "outliers"; and the dots indicate outliers. This figure was built using package *ggplot2* for R software (Wickham, 2009; R Core Team, 2019).

Journal Pre-proof

Tables

Region /Province	Natura 2000 SAC	Location	Coordinates		Depth (m)	Species	Observations	Code
Mediterranean, Almería	ES6110010	Terreros	37º21´0.12´´N	1º40´36.37´´W	5.5	*Posidonia oceanica*		TE.S
Mediterranean, Almería	ES6110010	Terreros	37º20´37.00´´N	1º39´10.60´´W	18.5	*P. oceanica*		TE.D
Mediterranean, Almería	ES6110010	Villaricos	37º15´18.93´´N	1º45´29.53´´W	15.9	*P. oceanica*	Chemically degraded	DE.I
Mediterranean, Almería	ES6110010	Palomares	37º12´27.13´´N	1º47´30.20´´W	10.2	*Cymodocea nodosa*		PA.I
Mediterranean, Almería	ES0000046	Aguamarga	36º56´15.66´´N	1º56´0.42´´W	4.8	*P. oceanica*		AG.S
Mediterranean, Almería	ES0000046	Aguamarga	36º56´10.20´´N	1º55´55.32´´W	10.8	*P. oceanica*		AG.I
Mediterranean, Almería	ES0000046	Aguamarga	36º55´59.40´´N	1º55´55.32´´W	18	*P. oceanica*		AG.D
Mediterranean, Almería	ES0000046	El Alquián	36º49´23.5´´N	2º23´8.04´´W	6.8	*C. nodosa*		BA.S
Alborán, Almería	ES6110019	Roquetas	36º47´15.50´´N	2º35´20.10´´W	1.5	*P. oceanica*		RO.S
Alborán, Almería	ES6110019	Roquetas	36º47´11.35´´N	2º35´24.[illegible]0´´W	0.7	*P. oceanica*	Chemically degraded, dead mat	RO.S-C
Alborán, Almería	ES6110019	Roquetas	36º47´12.2´´N	2º35´24.20´´W	1	*C. nodosa*		RO.S-CN
Alborán, Almería	ESZZ16003	Almerimar	36º41´51.72´´N	2º49´32.46´´W	4.5	*P. oceanica*		AL.S
Alborán, Granada	-	Melicena	36º44´53.99´´N	3º14´3.78´´W	4.2	*P. oceanica*	In decline	ME.S
Alborán, Málaga	ES6170030	Calaburras	36º29´26.60´´N	4º41´36.40´´W	0.5	*P. oceanica*	Dead mat with *C. nodosa* growing on top	CA.S-CN
Alborán, Málaga	ES6170030	Calaburras	36º29´26.60´´N	4º41´36.40´´W	0.5	*P. oceanica*	Dead mat	CA.S-C

Table 1: Summary of the stations studied. Natura 2000 SAC, Special Areas of Conservation under the European program Natura 2000 ID.

Journal Pre-proof

Code	Sampling date Month/ year	Compression %	Core length (cm)	Max age (cal. y BP)	Accretion rate top meter (mm y^{-1})	Dating method	C_{org} (gcm^{-3})	Clay (%)	Silts (%)	FSands (%)	MSands (%)	CSands (%)
TE.S	10/2016	20.4	88.7	930	1.09 ± 0.14	^{210}Pb, ^{14}C	0.0218	0.04	13.41	72.43	8.87	5.26
TE.D	10/2017	-	200	2992	0.99 ± 0.18	^{14}C	0.0830	0.31	15.69	33.58	31.07	19.30
DE.I	10/2016	15.9	157.2	3620	0.71 ± 0.15	^{210}Pb, ^{14}C	0.0096	0.27	23.18	30.70	19.98	25.86
PA.I	10/2017	14.3	147.9	217	7.57 ± 3.82	^{210}Pb	0.(025	.00	4.94	94.93	0.01	0.13
AG.S	10/2017	13.1	172.9	2044	1.88 ± 0.44	^{210}Pb, ^{14}C	0.(268	0.04	6.24	57.50	30.16	6.05
AG.I	10/2017	31.4	166.4	763	3.56 ± 0.92	^{210}Pb, ^{14}C	0.0138	0.18	16.15	78.01	2.61	3.03
AG.D	10/2017	11.3	136.8	3719	0.42 ± 0.05	^{210}Pb, ^{14}C	0.0191	0.30	20.64	41.58	14.51	22.93
BA.S	10/2016	9.9	117.3	355	4.71 ± 1.07	^{14}C	0.0025	0.03	13.95	85.81	0.00	0.20
RO.S	10/2016	41.5	137.7	1084	1.[illegible] ± 0.19	^{210}Pb, ^{14}C	0.0226	0.01	8.45	81.28	6.47	3.78
RO.S-C	10/2016	40.3	141.7	800	-	-	0.0279	0.01	7.61	87.70	3.10	1.57
RO.S-CN	10/2016	59.9	173.5	-	-	-	0.0015	0.00	0.68	78.30	1.62	16.84
AL.S	10/2017	0.8	106.9	1213	0.88 ± 0.12	^{14}C	0.0195	0.10	16.71	72.94	6.77	3.49
ME.S	10/2017	10.9	77.[illegible]	371	1.98 ± 0.85	^{210}Pb, ^{14}C	0.0133	0.02	8.58	45.12	26.68	19.59
CA.S	10/2017	21.2	[illegible].5-102.9	-	-	-	0.0173	0.00	4.48	57.89	12.00	25.63

Table 2: Main characteristics of the cores studied. FSands, MSands, and CSands stand for Fine, Medium and Coarse sands, respectively.

Journal Pre-proof

	PC1	PC2	PC3	PC4	PC5	Com
Rb	**0.92**	-0.04	-0.10	-0.02	0.04	0.85
Fe	**0.90**	-0.18	-0.07	0.10	-0.15	0.87
Zn	**0.79**	0.02	0.11	-0.08	0.19	0.69
K	**0.78**	0.25	0.00	-0.10	-0.02	0.68
Ti	**0.77**	-0.29	0.27	-0.05	-0.27	0.83
Al	**0.76**	-0.34	0.31	-0.11	-0.29	0.89
Zr	**0.73**	**-0.37**	0.07	0.12	0.13	0.71
Si	**0.58**	**-0.50**	**0.35**	-0.28	-0.27	0.86
C_{org}	**-0.48**	0.32	0.08	0.20	**0.35**	0.50
Mn	**0.47**	-0.28	-0.10	**-0.42**	-0.17	0.51
Sr	-0.07	**0.88**	0.21	-0.01	-0.06	0.83
FSand	0.06	**-0.78**	**0.37**	-0.26	0.01	0.82
Cl	-0.06	**0.75**	-0.07	0.04	0.29	0.66
Ca	-0.24	**0.72**	0.24	**-0.40**	-0.07	0.79
CSand	-0.07	**0.61**	**-0.50**	0.18	-0.27	0.74
MSand	**-0.37**	**0.47**	**-0.60**	0.09	0.16	0.75
Silt	**0.39**	-0.07	**0.67**	0.19	0.20	0.68
MS	0.23	-0.16	**-0.62**	0.06	0.07	0.47
Ni	-0.14	-0.10	-0.13	**0.69**	-0.16	0.55
Pb	**0.38**	0.22	0.10	**0.57**	0.06	0.52
Br	-0.32	0.06	0.05	**0.55**	**0.48**	0.64
S	0.02	-0.02	0.00	-0.06	**0.76**	0.58
Var %	27.51	18.28	9.30	7.99	6.97	
Ac. Var %	27.51	45.79	55.08	63.08	70.05	

Table 3: Loadings of chemical elements, magnetic susceptibility (MS), grain sizes (silts, FSand, MSand and CSand) and organic carbon density (C_{org}) for each component as yielded by the principal components analysis (PCA). Com: communality (total variance of each variable explained by the extracted components), Var. %: percentage of variance accounted for by each component; Ac. Var. %: cumulative variance**.** Loadings > 0.35 in bold.

Journal Pre-proof

Author contributions

Nerea Piñeiro-Juncal: Conceptualization; Data curation; Formal analysis; Investigation; Validation; Visualization; Roles/Writing - original draft; Writing - review & editing. **Elena Diaz-Almela**: Data curation; Formal analysis; Project administration; Writing - review & editing. **Carmen Leiva-Dueñas**: Formal analysis; Methodology; Writing - review & editing. **Ona Deulofeu**: Formal analysis. **Jaime Frigola**: Data curation; Formal analysis; Methodology; Writing - review & editing. **Montserrat Soler**: Data curation; Formal analysis; Writing - review & editing. **Antonio Martinez-Cortizas**: Data curation; Formal analysis; Methodology; Writing - review & editing. **Santiago Giralt**: Conceptualization; Data curation; Writing - review & editing. **Jordi Garcia-Orellana**: Data curation; Formal analysis; Writing - review & editing. **Miguel Ángel Mateo**: Funding acquisition; Project administration; Resources; Supervision; Writing - review & editing.

Journal Pre-proof

Declaration of interests

☒ The authors declare that they have no known competing financial interests or personal relationships that could have appeared to influence the work reported in this paper.

☐The authors declare the following financial interests/personal relationships which may be considered as potential competing interests:

Journal Pre-proof

Highlights

- There is a growing interest in seagrass soil formation processes.

- Fifteen cores of the two main Mediterranean seagrass species were sampled.

- Principal component analysis was used to summarize diverse geochemical proxies.

- Terrestrial influence explained 55% of the variance in soil texture and composition.

-The temporal variability in organic matter inputs affected C_{org} accumulation.

Journal Pre-proof

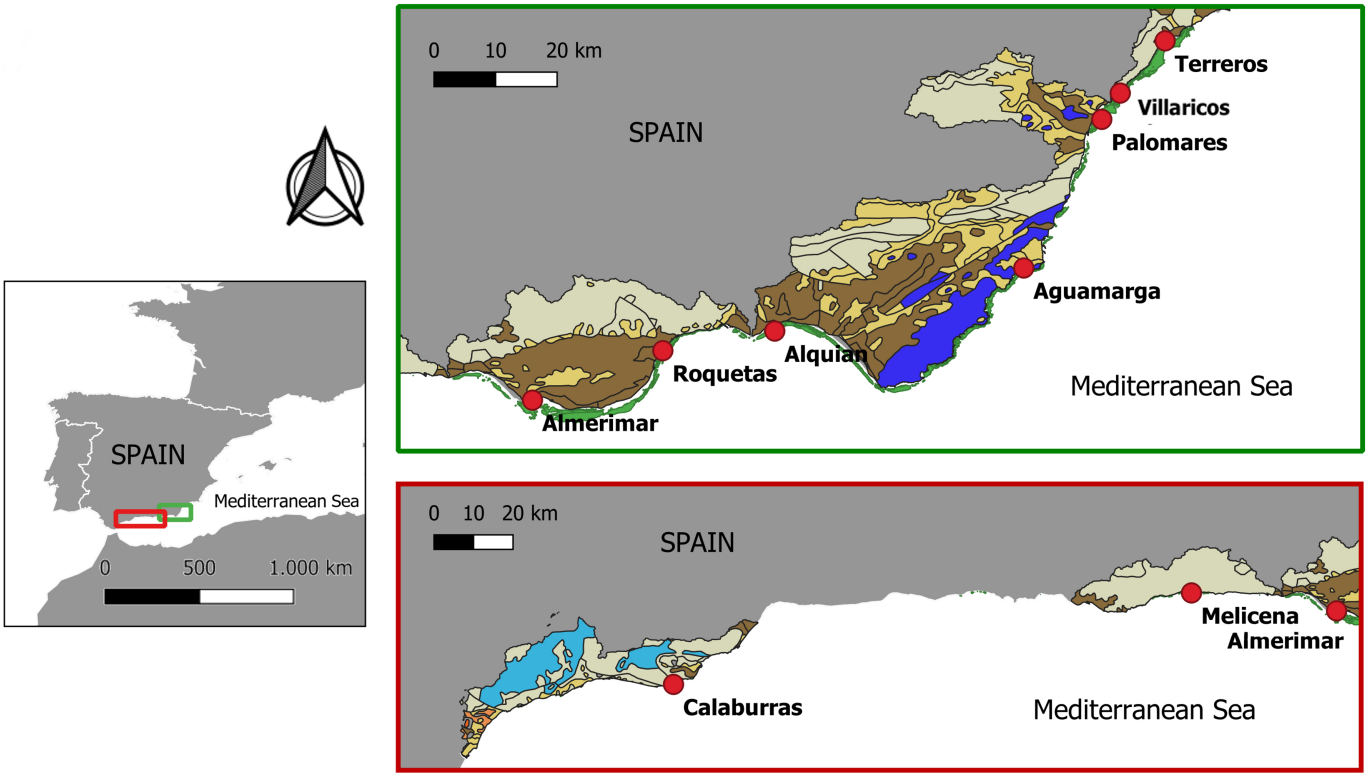
0 10 20 km
SPAIN
Terreros
Villaricos
Palomares
Aguamarga
Alquian
Roquetas
Almerimar
Mediterranean Sea
SPAIN
Mediterranean Sea
0 500 1.000 km
0 10 20 km
SPAIN
Melicena
Almerimar
Calaburras
Mediterranean Sea
Lithology
Sandstones, conglomerates, clays; limestone and evaporites
Limestones, dolomites and marls. Sandstones and conglomerates
Gravels, conglomerates, sands and silts
Mica schists, phyllites, sandstones, marbles, limestones, dolomites and marls
Serpentinites and peridotites. Basic and ultrabasic rocks
Vulcanites and volcanoclastic rocks
Seagrass meadows
Seagrass meadows

Figure 1

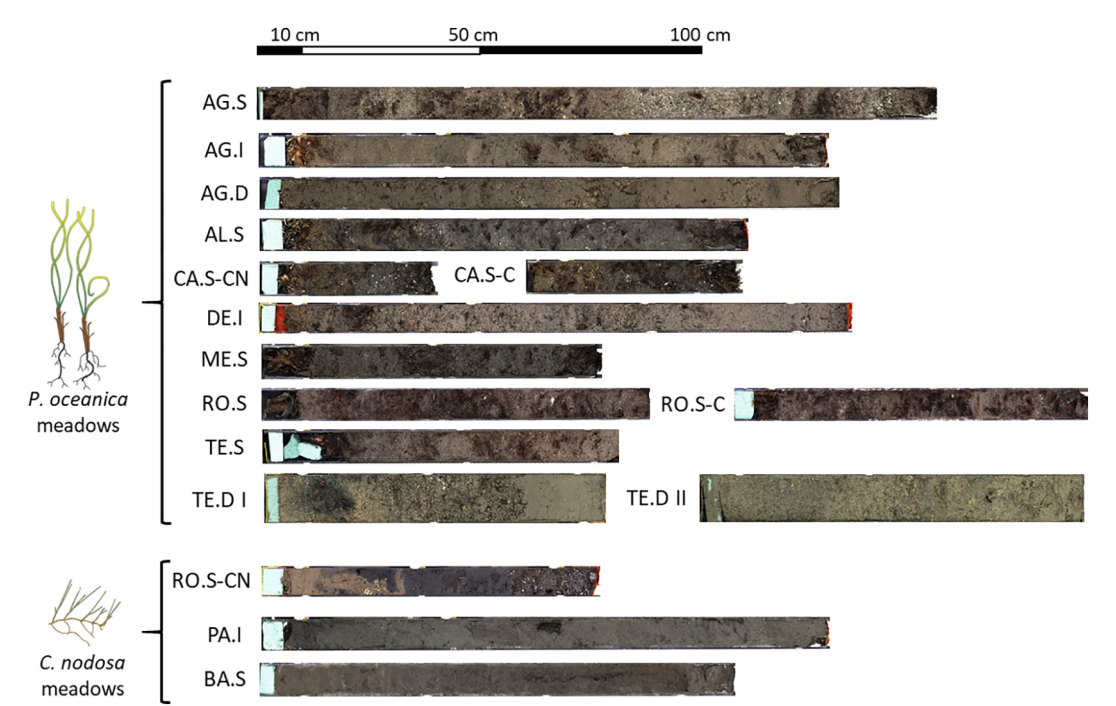
10 cm
50 cm
100 cm
AG.S
AG.I
AG.D
AL.S
CA.S-CN
CA.S-C
DE.I
ME.S
RO.S
RO.S-C
TE.S
TE.D I
TE.D II
P. oceanica meadows
RO.S-CN
PA.I
BA.S
C. nodosa meadows

Figure 2

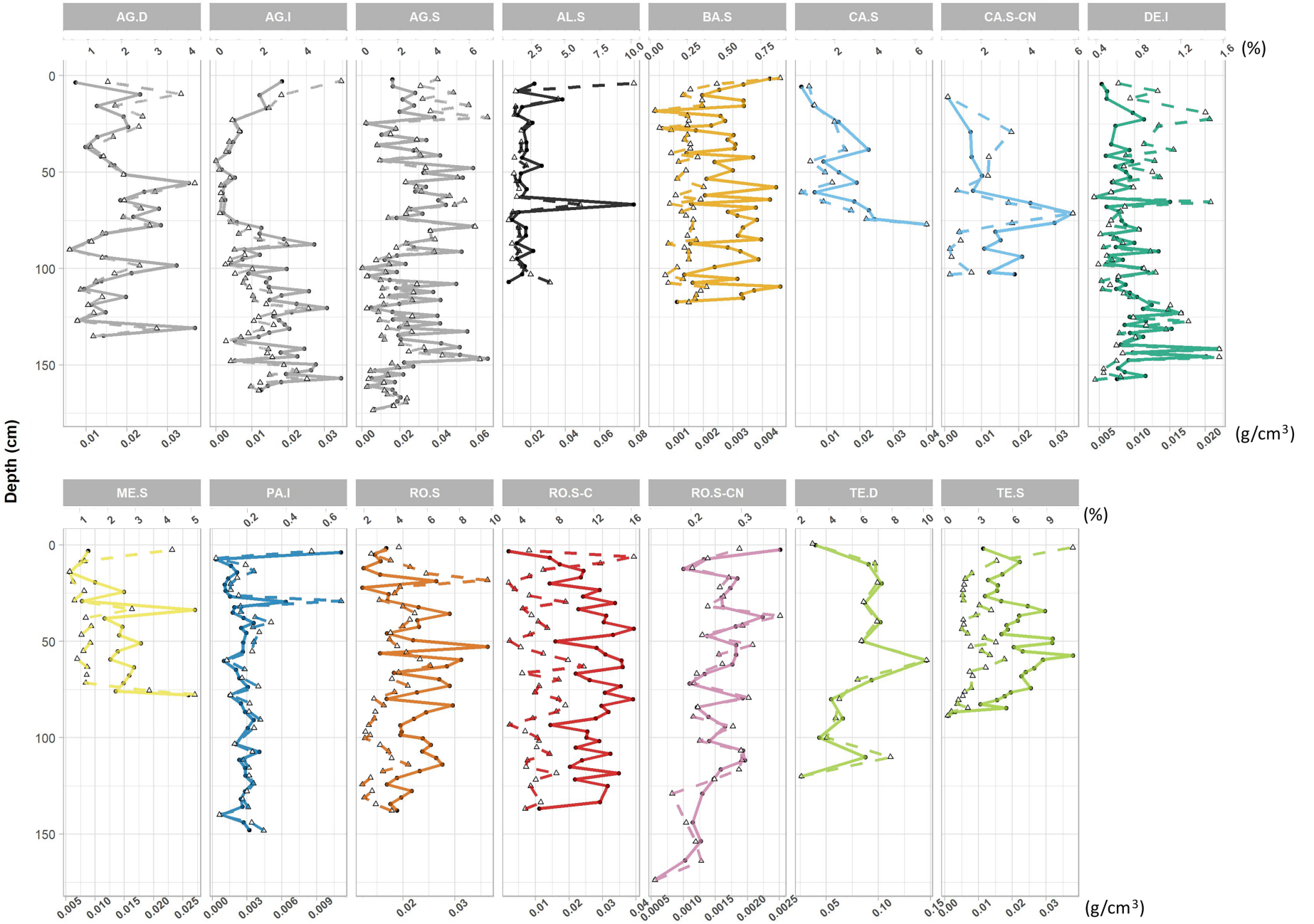
AG.D
AG.I
AG.S
AL.S
BA.S
CA.S
CA.S-CN
DE.I
ME.S
PA.I
RO.S
RO.S-C
RO.S-CN
TE.D
TE.S
Depth (cm)
(%)
(g/cm³)
Organic Carbon: solid line g/cm³; dashed line %.

Figure 3

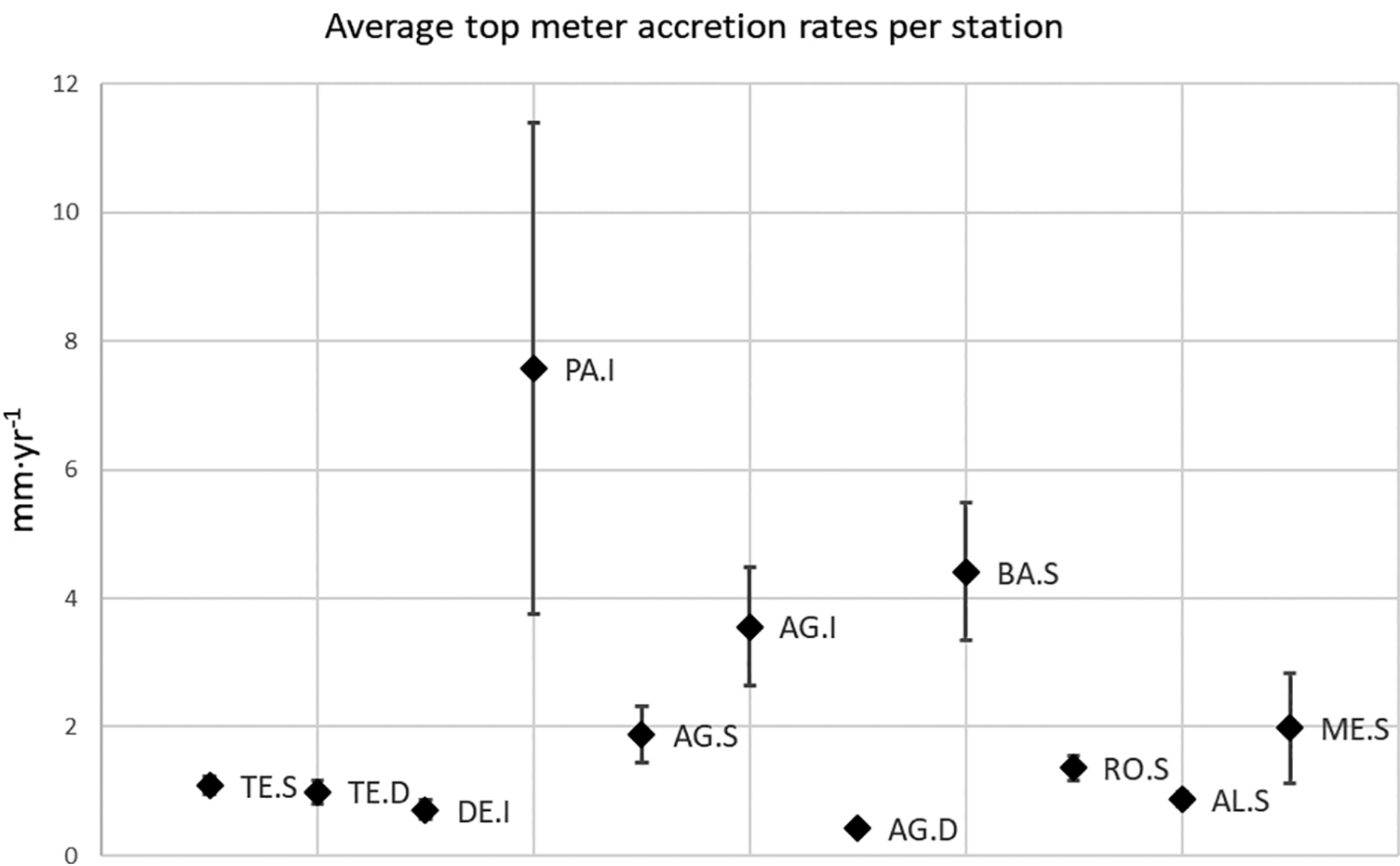
Average top meter accretion rates per station
12
10
8
6
4
2
0
mm·yr-1
PA.I
TE.S
TE.D
DE.I
AG.S
AG.I
AG.D
BA.S
RO.S
AL.S
ME.S

Figure 4

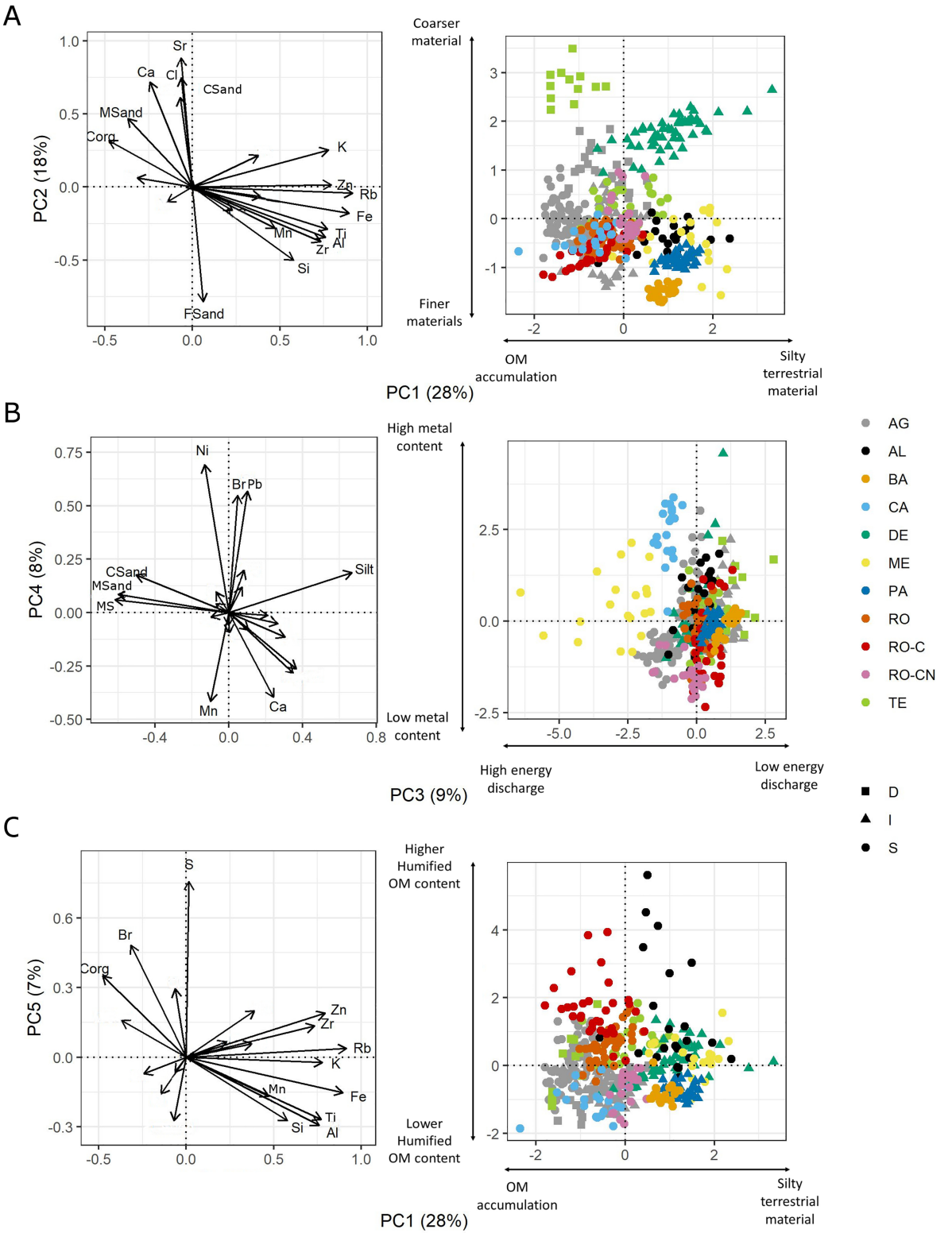
A
Sr
Ca
Cl
CSand
MSand
Corg
K
Zn
Rb
Fe
Mn
Ti
Zr
Al
Si
FSand
PC2 (18%)
Coarser material
Finer materials
OM accumulation
Silty terrestrial material
PC1 (28%)
B
Ni
Br
Pb
CSand
MSand
MS
Silt
Mn
Ca
PC4 (8%)
High metal content
Low metal content
High energy discharge
Low energy discharge
PC3 (9%)
AG
AL
BA
CA
DE
ME
PA
RO
RO-C
RO-CN
TE
D
I
S
C
S
Br
Corg
Zn
Zr
Rb
K
Mn
Fe
Ti
Si
Al
PC5 (7%)
Higher Humified OM content
Lower Humified OM content
OM accumulation
Silty terrestrial material
PC1 (28%)

Figure 5

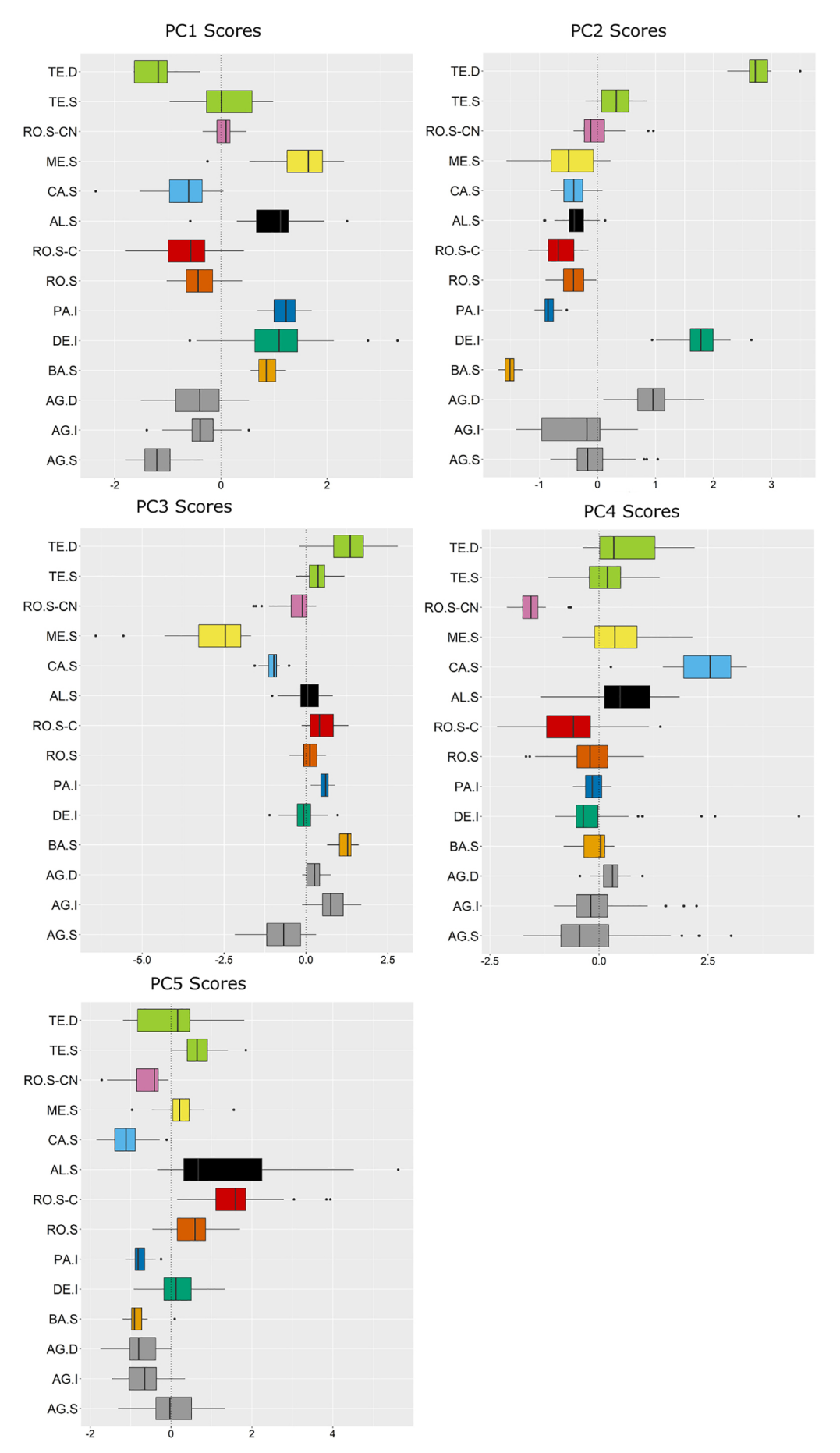
PC1 Scores
TE.D
TE.S
RO.S-CN
ME.S
CA.S
AL.S
RO.S-C
RO.S
PA.I
DE.I
BA.S
AG.D
AG.I
AG.S
-2
0
2
PC2 Scores
-1
0
1
2
3
PC3 Scores
-5.0
-2.5
0.0
2.5
PC4 Scores
PC5 Scores
4

Figure 6